Photoinduced luminescence from the noble metals and its enhancement on roughened surfaces

G. T. Boyd,* Z. H. Yu, and Y. R. Shen
Department of Physics, University of California, Berkeley, California 94720
and Materials and Molecular Research Division, Lawrence Berkeley Laboratory,
University of California, Berkeley, California 94720
(Received 23 December 1985)

Single-photon- and multiphoton-induced luminescence spectra were obtained from clean samples of silver, copper, and gold with both smooth and rough surfaces. The spectra reveal new features which are correlated with interband transitions at selected symmetry points in the Brillouin zone. Calculating luminescence spectra based on simplified models of the band structures of the noble metals and taking into account the Fresnel local-field corrections, we find qualitative agreement with the observed spectra from smooth samples. The agreement between theory and experiment is less satisfactory for rough samples. The influence of surface roughness on the luminescence is largely attributable to local-field enhancement in the rough surface protrusions.

I. INTRODUCTION

Photoluminescence has been used extensively in the study of inelastic scattering processes in semiconductors. Its use in characterizing carrier relaxation and the band structure of metals was first suggested by the discovery of photoluminescence from copper and gold by Mooradian.[1] In the original experiment, monochromatic light at 4880 Å was used to excite a luminescence spectrum which displayed a broad peak centered near the interband absorption edge of the metals. The peak was attributed to direct radiative recombination of electrons near the Fermi level with holes in the first *d* band. Many of the essential details of this mechanism, such as the excited-electron- and hole-population distributions, the specific regions in the Brillouin zone where the recombination takes place, and the reabsorption of the emitted luminescence, have not been discussed. By Mooradian's hypothesis, additional peaks in the luminescence spectra should result if higher-energy excitations are used to create holes in lower-lying *d* bands. The peak energies would correspond to the energy difference between the Fermi level and the various *d* bands at certain symmetry points. Despite the possible usefulness of this technique as a band-structure probe, luminescence from metals has remained relatively unexplored since Mooradian's original experiment.[2,3]

Renewed interest in luminescence from metals came with a number of discoveries related to noble metals with roughened surfaces. Much excitement was generated by the observation of an enormous enhancement in the Raman cross section of molecules adsorbed to a roughened noble-metal surface.[4] In addition to the sharp Raman peaks from the adsorbed molecules, a broadband luminescence background was observed.[5] Experiments in ultrahigh vacuum showed that at least part of the luminescence must originate from the substrates.[6–8] This background currently constitutes the fundamental noise limit for surface-enhanced Raman scattering (SERS). It is now widely accepted that for optical processes the primary role of the roughness in metals is to enhance the local optical fields via localized plasmon resonances, and thus improve the efficiency of light absorption and emission. This so-called local-field effect is responsible for a major part of the Raman enhancement,[3] and for a variety of other effects including the enhancement of luminescence of dyes adsorbed to roughened metals,[9,10] and the increase in photochemical activity of adsorbates on roughened metals.[11] Local-field effects are also used to explain the enhancement of light emission from tunnel junctions with roughened noble-metal electrodes.[12–14] The broadband spectra from these junctions are strongly influenced by the dispersion of the localized plasmon resonances. It is expected that the same resonances will affect the photoinduced luminescence spectra as well. A comparison of such spectra from rough and smooth metal samples would provide a probe of the plasmon dispersion and a test for the local-field models.

Luminescence may also be excited by multiphoton absorption. Multiphoton-induced luminescence was first observed as a broadband background in second-harmonic–generation (SHG) measurements on roughened noble metals.[15] Preliminary studies revealed significant differences between the broadband emission excited by single-photon and multiphoton absorption.[16] In the former case, the luminescence intensity rises with increasing emission energy towards the pronounced interband peak, for both rough and smooth surfaces. However, the multiphoton-induced luminescence from the roughened surfaces dramatically decreases with increasing emission energy, and displays no detectable peak. Some authors have speculated that the missing peak is the result of two-photon selection rules.[17] The mixed parity of the *d* and *sp* bands for these metals, however, weakens this argument. On the other hand, because the multiphoton luminescence was observed from a roughened metal, the effects of the localized plasmon resonances must be included in the interpretation of the spectra. In particular, the multiphoton luminescence is more sensitive to the local fields than the single-photon luminescence. Since the local fields are strongest just outside the metal surface,

multiphoton-induced emission from the surface atoms may dominate over that from the bulk, yielding different luminescence spectra from the bulk.

In addition to the many unexplored theoretical questions regarding metal luminescence, much of the previous experimental data may have been complicated by emission from surface contaminants, since many of the spectra were obtained from samples exposed to the air or immersed in an electrochemical cell. Unless precautions against contamination are taken, it is possible that the photoinduced luminescence from a roughened sample may include enhanced luminescence from adsorbates. Another complexity in the existing experimental results is the response of the various detection systems. Since the emission energies may range over many electron volts, a correction for this dispersion is essential to obtain the true luminescence spectra.

This paper presents spectra of single-photon- and multiphoton-induced luminescence obtained from clean films of sliver, copper, and gold, prepared and maintained in high vacuum (10^{-9} Torr). All spectra were corrected for the dispersion of the detection system. Furthermore, in order to probe the lower-lying d bands, higher excitation energies than those of previous experiments were used. New features appear in the single-photon-induced luminescence spectra as a result. When possible, spectra were obtained from both smooth and rough surfaces, with the same surface morphology for all metals. The multiphoton-induced spectra could be detected only from the roughened samples.

The details of the sample preparation, the excitation source, and the detection system are given in the next section. Following this, we present the single-photon-induced luminescence spectra from smooth samples of silver, copper, and gold, and include a brief physical interpretation of the results. The effects of roughness on these spectra are then described and discussed. The multiphoton-induced luminescence spectra from the rough samples are then presented, and contrasted with the single-photon-induced luminescence. A more detailed interpretation of all the spectra is given in the Discussion section. There we present a simple calculation which correlates the spectral peaks with interband recombination at selected symmetry points in the Brillouin zone. The excited-electron- and hole-energy distributions are deduced from the data to provide insight into the carrier-relaxation process. The effects of roughness on the luminescence are estimated with a simple local-field model and compared with the data. We then examine the multiphoton-induced luminescence spectra, stressing the effects of local plasmon resonances in interpreting the spectra. We conclude with a summary of the results and an evaluation of photoluminescence as a band-structure probe for metals.

II. EXPERIMENT

A. Sample preparation

In an effort to eliminate possible contributions to the luminescence from surface adsorbates, the samples were prepared and maintained in high vacuum (10^{-9} Torr). The samples were made by evaporating approximately 1000 Å of high-purity metals (99.998%) onto roughened and smooth substrates. The pressure during the evaporation did not exceed 10^{-7} Torr. Before each evaporation, the chamber and the source filament were out-gassed at high temperature (200 °C for the chamber, 800 °C for the filament) for 24 h. Several measurements were performed to establish that these films were sufficiently clean: (1) No surface-enhanced Raman peaks were detected from these samples, indicating that they were free from organic adsorbates. (2) Rough samples in air produced as much as 100 times the two-photo-induced luminescence as these samples in vacuum. (3) Gold films prepared under similar conditions have been shown to be free of surface adsorbates.[18] On the other hand, the luminescence intensity from our Au films exceeded that from Ag and Cu, which under these conditions could still be contaminated by surface oxide.[19] This indicates that the minor surface contamination on Ag and Cu contributed negligibly to the luminescence, if at all. The substrate used was a glass slide, half of which was roughened by a chemical etching technique.[20] The evaporated films conformed to the substrate morphology to produce a metal surface, half of which was rough and half of which was smooth (Fig. 1). Electron photomicrographs of the rough samples revealed a surface covered with structures 100–1000 Å in size. The same roughness morphology was guaranteed for each metal by chemically removing the metal films and reusing the same substrate.

B. Optical arrangement and detection system

A Q-switched Nd:YAG (YAG denotes yttrium aluminum garnet) laser and a harmonic generator were used to provide excitation energies of 1.17, 2.34, 3.50, and 4.67

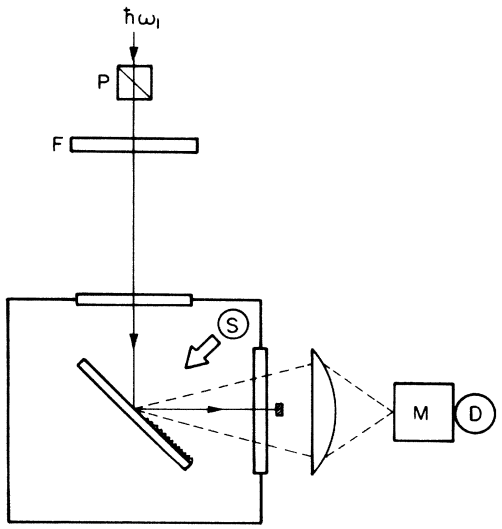

FIG. 1. Diagram of the experimental apparatus. Noble metals were evaporated from source (S) onto smooth and roughened substrates in a high-vacuum chamber. The excitation beam was p-polarized by a prism (P) and passed through a spectral filter (F). The luminescence was focused onto a monochromator (M) and detected with a photomultiplier (D).

eV. The incoming beam was p-polarized, having a nearly Gaussian spatial profile, and was incident at 45° to the sample surface. The intensities used were typically 1—10 MW/cm^2, with pulse durations of 8 ns. The luminescence was collected at 90° to the incident beam by an $f/1.5$ fused-quartz lens, and focused either onto a triple monochromator [80 Å full width at half maximum (FWHM)] in the case of the one-photon-induced luminescence, or, for the weaker multiphoton-induced spectra, onto a single monochromator (100 Å FWHM) equipped with spectral filters. The monochromators were scanned in 10-nm intervals. Any incident light which was specularly reflected was removed by a nonluminescing absorber. Tests using the monochromators and spectral filters were routinely performed to insure that the signals included no elastically scattered light. Additional spectral filters were used in some cases to avoid higher-order diffraction from the monochromator gratings. A photomultiplier which had a broad spectral response (Hammatsu H955), was used as the detector. The electrical signal was processed by a gated integrator, interfaced to a microcomputer which averaged each spectral point over at least 1500 laser pulses.

Absolute spectra were obtained by compensating the data for the dispersion of the detection system, measured with a calibrated tungsten-halogen lamp. All final spectra were repeatable typically to within 20%.

III. RESULTS

A. Single-photon-excited spectra from copper

1. Smooth sample

The spectra of single-photon-induced luminescence, from the smooth sample of Cu, are shown as solid curves in Figs. 2(a)—2(c) at increasing excitation energies. At the lowest excitation energy [Fig. 2(a)], the spectrum consists of a single peak at 2.15 eV, in good agreement with the spectra obtained by others.[1-3] The quantum efficiency of the luminescence was approximately 10^{-10}, which is also in agreement with earlier measurements.[1] The peak has been attributed by Mooradian to recombination radiation between electrons near the Fermi level and photoexcited holes in the first d band.

At a higher excitation energy of 3.50 eV, we observe an additional peak in the luminescence at 2.90 eV [Fig. 2(b)]. Since 3.50-eV photons have enough energy to excite electrons from the second d band of Cu,[21] we will attribute the second peak to recombination radiation between electrons near the Fermi level and holes in the second d band. The spectrum also displays a slight rise in intensity toward the excitation energy. Various tests were made to assure that this is definitely from luminescence instead of elastic scattering. Because there are no further d band transitions which can be reached by 3.50-eV photons,[21] we have to attribute it to recombination radiation between photoexcited electrons above the Fermi level, and holes in the first and second d bands.

At the highest excitation energy of 4.67 eV, the luminescence signal detected from smooth Cu was 30 times weaker than that obtained with 2.34-eV excitation, and no spectral structure could be clearly discerned.

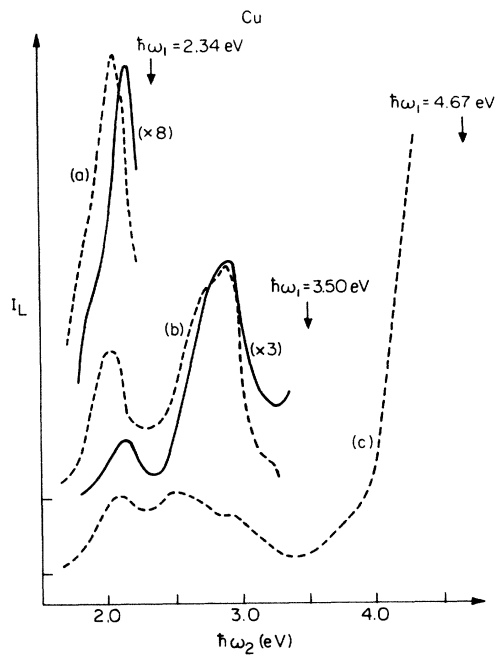

FIG. 2. Luminescence spectra from smooth (——) and rough (— — —) samples of copper induced by incident energies of (a) 2.34, (b) 3.50, and (c) 4.67 eV. Spectra from the smooth surfaces are enhanced by the factors indicated.

2. Rough sample

The effects of roughness on the one-photon luminescence were also investigated. The spectra from the rough Cu film are shown as dashed curves in Figs. 2(a)—2(c). At the lowest excitation energy [Fig. 2(a)], the spectral peak is 8 times larger than that from the smooth sample, and is shifted to a lower energy. This shift of the emission peak is a natural consequence of localized plasmon resonances which produce an increasingly large surface enhancement as the emission energy decreases.

At the excitation of 3.50 eV [Fig. 2(b)], again because of the localized plasmon resonances, only the low-energy peak appears to have shifted to lower energies from that of the smooth sample, in addition to being more intense. The rise in intensity near the excitation energy, which is evident from the smooth sample, is absent in the rough sample spectrum. This could be due to roughness quenching of the photoexcited electrons above the Fermi level. At the excitation energy of 4.67 eV, however, roughness quenching is apparently insufficient to remove the tail in the spectrum of the rough sample, seen in Fig. 2(c). We also observe in this spectrum a broad feature from 1.9 to 3.3 eV containing several weak peaks, which are shifted from those of Fig. 2(b).

B. Single-photon-excited spectra from gold

1. Smooth sample

The one-photon luminescence spectra from the smooth sample of Au are shown as solid curves in Figs. 3(a)—3(c).

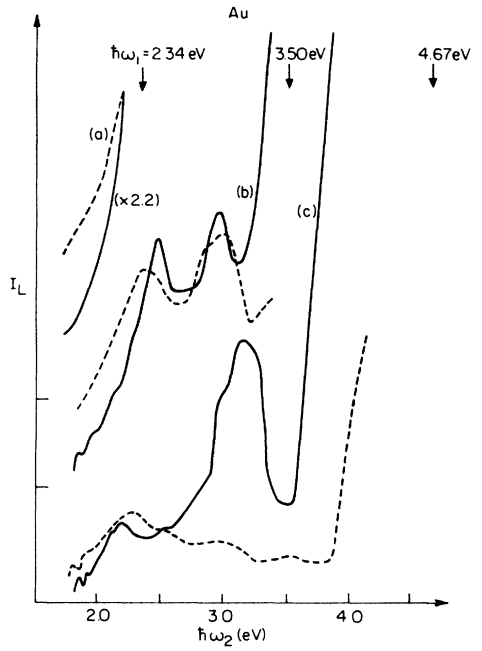

FIG. 3. Luminescence spectra from smooth (——) and rough (— — —) samples of gold induced by incident energies of (a) 2.34 eV, (b) 3.50, and (c) 4.67 eV. The spectrum in (a) from smooth gold is enhanced by 2.2

The peak which has been observed by other investigators, at 2.4 eV,[1,22] is just above our first excitation energy of 2.34 eV. The spectrum shown in Fig. 3(a) is evidently the tail of this peak, which monotonically decreases with decreasing emission energy. At the higher excitation energy of 3.50 eV, a peak appears at 2.50 eV in addition to one at 2.95 eV. As with Cu, we will attribute these peaks, as well as the weak structure near 1.8 eV, to recombination between electrons near the Fermi level and holes in the top two *d* bands. The sharp rise toward the excitation energy is also evident as in the case of Cu.

At the highest excitation of 4.67 eV, many new features appear in the spectrum [Fig. 3(c)]. Pronounced peaks at 2.2 and 3.2 eV are evident, with additional features at 1.9, 2.55, and 3.0 eV. The rise towards the excitation energy is also very strong. Most of the new features will be assigned to transitions involving holes created in the three *d* bands.

2. Rough sample

The one-photon-induced luminescence spectra from the rough sample of Au are shown as dashed curves in Figs. 3(a)—3(c). For the excitation energies of 2.34 eV, as with Cu, the roughness broadens the luminescence, especially at energies below the interband absorption edge. For the excitation energy of 4.67 eV [Fig. 3(c)], the major spectral feature near 3.2 eV is strongly suppressed. In all cases, the sharp increase of luminescence towards the excitation energy observed from smooth samples is strongly suppressed, presumably due to roughness quenching.

C. Single-photon-excited spectra of silver

1. Smooth sample

No luminescent peak can be expected from excitation below 3.5 eV for Ag. With the excitation at 4.67 eV, the spectrum, shown as a solid curve in Fig. 4, consists of a single peak, extending from 3.6 to 3.9 eV, and a shoulder above 4 eV. An examination of the band-structure calculations for Ag,[21] and the photoabsorption[23] and photothermal data[24,25] from the literature, reveals that the peak position is far from any direct Fermi-level—to—*d*-band transition. However, the volume- and surface-plasmon energies for Ag are in close correspondence with the observed peak.[23]

2. Rough sample

The one-photon-induced luminescence from rough Ag is shown in Fig. 4 (dashed curve). The essential effect of the roughness is to broaden the luminescence peak to energies as low as ≈ 3 eV. We will attribute the broadening to surface plasmons. It is well documented that surface-plasmon emission for Ag may be extended to these energies by roughening the surface.[26]

D. Multiphoton-excited spectra

Photoluminescence was also induced by multiphoton absorption. The resulting spectra from the rough samples of Cu, Au, and Ag are shown as solid curves in Fig. 5. No multiphoton-induced luminescence could be detected from any of the smooth samples.

All the spectra exhibit a second-harmonic, and in some cases, a third-harmonic peak resulting from surface harmonic generation. The broadband luminescence in each spectrum rises monotonically with decreasing emission energy.

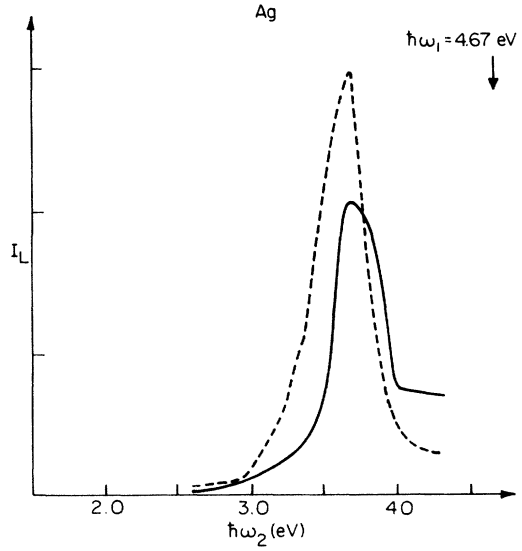

FIG. 4. Luminescence spectra from smooth (——) and rough (— — —) samples of silver induced by an incident energy of 4.67 eV.

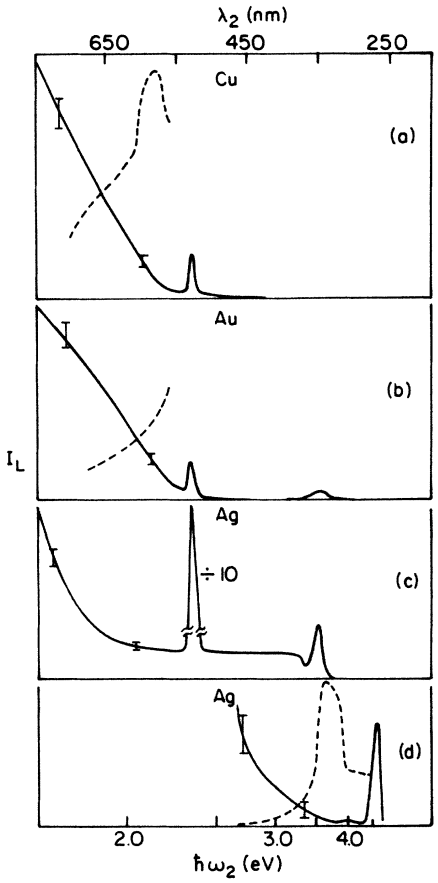

FIG. 5. Multiphoton-induced luminescence spectra from rough samples of Cu, Au, and Ag (——). Dashed curves show corresponding one-photon-induced spectra from smooth samples, taken from Figs. 2 and 4. Spectra (a)—(c) were obtained with laser excitation at 1.7 eV and spectrum (d) was obtained with excitation at 2.34 eV.

The number of photons involved in the multiphoton excitation can be inferred from the high-energy cutoff of the luminescence spectrum. For Cu and Au, at an excitation energy of 1.17 eV, the cutoff is at the two-photon energy, implying that the luminescence was initiated by two-photon absorption. To confirm this, the power dependence of the luminescence (as well as the second harmonic) was obtained, and found to be quadratic to within experimental error. For Ag, at an excitation of 1.17 eV, the luminescence extends continuously to the three-photon energy, implying its initiation by three-photon absorption. For an incident energy of 2.34 eV, the luminescence from Ag cuts off at an energy which implies two-photon absorption.

The one-photon-induced luminescence spectra from the smooth samples are reproduced as dashed curves in Fig. 5, for comparison. The peaks in the one-photon spectra of Cu and Ag are not apparent from the two-photon-excited spectra [Figs. 5(a) and 5(d)]. In addition, for all three metals, the one-photon luminescence decreases towards the low emission energies, while for the two-photon luminescence it increases. This can be attributed to the dispersion of the localized plasmon resonances on the rough surface.

IV. DISCUSSION

Our discussion of the photoluminescence spectra proceeds in several steps. We begin in subsection A by developing an expression for the luminescence resulting from direct transitions. A detailed comparison between the predictions and the data is then given in subsection B. The luminescence from the rough samples is treated in subsection C by replacing the local fields of the smooth surface with those of the rough surface, derived from a simple model. The results are compared with the observed spectra in subsection D for both the single-photon and multiphoton-induced luminescence.

A. General theory

Photoluminescence in solids is a three-step process involving photoexcitation of an electron-hole pair, the relaxation of the excited electrons and holes, and finally emission from the electron-hole recombination. The process is diagrammed in Fig. 6(a) between two representative bands for Au. We shall consider only direct transitions in the absorption and emission processes.

We may express the single-photon-induced luminescence from a slab of width dz at a depth z into the metal as

$$I_L(\omega_2)dz = I(\omega_1,z)Y_{1\text{abs}}Y_R Y_{\text{em}}dz\,, \tag{1}$$

where ω_2 and ω_1 are the luminescence and incident frequencies, respectively, $I(\omega_1,z)$ is the excitation intensity at ω_1 at a depth z, $Y_{1\text{abs}}$ is the probability for a single-photon absorption at ω_1, Y_R is the probability of relaxation of the electrons and holes from the excited states to the emitting states, and Y_{em} is the emission probability of radiative recombination at ω_2. The excitation intensity is given by

$$I(\omega_1,z) = I_0(\omega_1)\,|L(\omega_1)|^2 \exp[-\alpha(\omega_1)z]\,, \tag{2}$$

where $I_0(\omega_1)$ is the source intensity, $|L(\omega_1)|^2$ is the Fresnel transmission coefficient at ω_1, and α is the absorption coefficient. For two-photon-induced luminescence, $I(\omega_1,z)Y_{1\text{abs}}$ becomes $I^2(\omega_1,z)Y_{2\text{abs}}$, where $Y_{2\text{abs}}$ is the two-photon—absorption probability at $2\omega_1$.

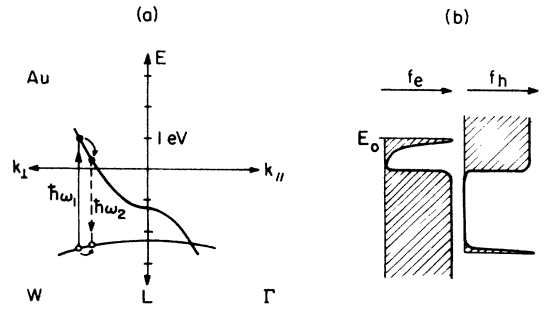

FIG. 6. (a) Partial band structure of Au at the L symmetry point showing excitation and emission paths. The band energies are relative to the Fermi level. (b) Electron and hole distribution functions used in the calculation. E_0 is the electron energy after excitation by the incident photons.

The direct absorption of photons at ω_1 will promote electrons from bands below the Fermi level into bands above the Fermi level at all points in the Brillouin zone where the band-energy separation is $\hbar\omega_1$. The theory for direct photoabsorption in the noble metals is treated in Refs. 21 and 24, and need not be reproduced here. After the absorption, the electrons and holes will relax from their initial excited states to new energy states, via the many scattering processes in the noble metals.[27] The luminescence results from the radiative recombination of these relaxed carriers. We will account for the relaxation by assuming a simple energy distribution of the relaxed electrons and holes in the calculation for the emission probability.

The probability of emission at ω_2 will be proportional to the total radiative recombination rate between all electrons and holes with an energy difference of $\hbar\omega_2$. If we designate the energy and wave vector of the Bloch state to which the electrons relax as E and $\mathbf{k}$, respectively, then from Fermi's golden rule for spontaneous emission from direct recombination (into a solid angle $d\Omega$ and bandwidth $d\omega_2$), we have

$$Y_{\rm em} \propto \omega_2 d\omega_2 d\Omega \, |L(\omega_2)|^2 \exp[-\alpha(\omega_2)z] \times \int\int \{ |\mathbf{p}_2|^2 \delta[E - E_U(\mathbf{k})] \delta[E - \hbar\omega_2 - E_L(\mathbf{k})] f_e(E) f_h(E - \hbar\omega_2) \} dE \, d^3\mathbf{k}, \quad (3)$$

where E_U and E_L are the energies of the upper electron and lower hole bands, respectively, $\mathbf{p}_2$ is the momentum matrix element between the bands, and $|L(\omega_2)|^2$ is the Fresnel transmission coefficient at ω_2. The factor $\exp[-\alpha(\omega_1)z]$ accounts for the absorption of the outgoing light within the metal. The functions f_e and f_h are the electron- and hole-population distributions, respectively, which result from the excitation and relaxation processes. These distribution functions are difficult to calculate from first principles, because they depend on the complex scattering processes in the metal. However, we expect the electron and hole populations to diminish continuously away from their initially excited states. For simplicity, we assume that these populations decay exponentially as the electrons sink down the upper band and the holes float up the lower band. If we designate the initial excited-state energy of the electrons as E_0, then

$$f_e(E) = F_D(E) + \Theta(E - E_0)\exp[(E - E_0)/\delta_e], \quad (4)$$

where

$$F_D(E) = [1 + \exp(E/kT)]^{-1}$$

is the Fermi-Dirac distribution, the unit step function $\Theta(x)$ is zero for $x < 0$ and unity for $x > 0$, and δ_e is an adjustable parameter representing the exponential width. The hole distribution is similarly written as

$$f_h(E_h) = 1 - F_D(E_h) + \Theta(E_{0h} - E_h)\exp[(E_{0h} - E_h)/\delta_h], \quad (5)$$

where the hole energy is $E_h = E - \hbar\omega_2$, $E_{0h} = E_0 - \hbar\omega_1$, and δ_h is also an adjustable exponential width. These functions are plotted in Fig. 6(b). The exponential terms in f_e and f_h are used to fit the observed rise in the luminescence intensity near the excitation energy. The rise is attributed to radiative recombination of excited electrons above the Fermi level with the excited holes in the lower band.

Further simplifications in the calculation of $Y_{\rm em}$ can be made. The integration over the Brillouin zone may be approximated by considering only those regions close to the symmetry points, since they will contribute the largest joint density of states for emission. We also need only consider the regions where the band pairs have an energy difference no greater than the excitation energy. In addition, we will ignore those regions in which the excited electrons and holes would scatter in different $\mathbf{k}$ directions such that direct recombination would not be possible. After an examination of the calculated band structures of the noble metals,[21] it is apparent that, for the excitations used in this experiment, these restrictions limit us to regions near the X and L symmetry points for all the noble metals. We will further assume that the momentum matrix elements are independent of $\mathbf{k}$ over such regions. This latter approximation has been used successfully in the calculation of the dielectric constants of the noble metals.[21,24]

The emission spectrum is estimated by evaluating $Y_{\rm em}$, using the assumed electron and hole distribution functions in Eqs. (4) and (5). After combining Eqs. (1)–(5) and integrating over z, we have, with the above approximations,

$$I_L(\omega_2) \propto F(\omega_1,\omega_2) \int dE[D(E,\hbar\omega_2) f_e(E) f_h(E - \hbar\omega_2)], \quad (6)$$

where

$$F(\omega_1,\omega_2) = \omega_2 |L(\omega_1)|^2 |L(\omega_2)|^2 z_0(\omega_1,\omega_2),$$

$$z_0(\omega_1,\omega_2) = 1/[\alpha(\omega_1) + \alpha(\omega_2)],$$

and

$$D(E,\hbar\omega_2) = \int_{L,X} d^3\mathbf{k} \, \delta[E - E_U(\mathbf{k})] \delta[E - \hbar\omega_2 - E_L(\mathbf{k})]. \quad (7)$$

Rosei evaluates $D(E,\hbar\omega_2)$ by writing the energy of the Bloch state near the L and X symmetry points as[24]

$$E_i(\mathbf{k}) = \Delta_i + \hbar^2 k_1^2/2m_{1i} + \hbar^2 k_2^2/2m_{2i}, \quad (8)$$

where Δ_i is the energy of the ith band at the symmetry point, measured from the Fermi level, $\mathbf{k}_1$ is the electron wave factor pointing from the L or X symmetry point to Γ, $\mathbf{k}_2$ is perpendicular to $\mathbf{k}_1$, and m_{1i} and m_{2i} are the band masses. Equation (7) then becomes

$$D(E,\hbar\omega_2) \propto [E - E_1(\hbar\omega_2)]^{1/2}, \quad (9)$$

where

$$E_1(\hbar\omega)=\Delta_U+m_{2L}(\Delta_U-\Delta_L-\hbar\omega)/(m_{2U}-m_{2L})\ . \quad (10)$$

The limits of integration in Eq. (6) are given by

$$E_{\min}=E_1(\hbar\omega_1)-\hbar\omega_1+\hbar\omega_2$$

and

$$E_{\max}=E_1(\hbar\omega_1)$$

for $\hbar\omega_2\geq\Delta_U-\Delta_L$, while for $\hbar\omega_2<\Delta_U-\Delta_L$,

$$E_{\max}=\Delta_U+(\Delta_U-\Delta_L-\hbar\omega_2)m_{1L}/(m_{1U}-m_{1L})\ .$$

B. Calculated single-photon excitation spectra and comparison with experiment

We evaluate the single-photon excitation spectra from Eq. (6) by first evaluating the factor $F(\omega_1,\omega_2)$, containing the Fresnel transmission coefficients at ω_2, and the effective absorption depth, z_0. For the smooth surface, with p-polarized incident light, the dominant fields inside the metal will be parallel to the surface. The relevant Fresnel coefficient is then[28]

$$L(\omega)=2\cos\theta_m/[\epsilon_m^{1/2}(\omega)\cos\theta+\cos\theta_m]\ , \quad (11)$$

where ϵ_m is the metal dielectric constant, θ is the angle of incidence, and θ_m is the angle of refaction in the metal. Figure 7 shows a plot of

$$F=\omega_2\,|L(\omega_1)|^2\,|L(\omega_2)|^2 z_0(\omega_1,\omega_2)$$

versus ω_2, for $\theta=45°$ and $\hbar\omega_1=3.50$ eV. The necessary dielectric constants were obtained from Ref. 23. We see from the figure that, for Cu and Au, F shows a peak around the onset of the interband transitions. The peak for Ag which appears at 3.78 eV corresponds to the excitation of a volume plasmon, where $\mathrm{Re}(\epsilon_m)=0$. Such a peak is expected to strongly affect the spectrum from Ag.

The integral in Eq. (6) was evaluated using band parameters obtained from the calculations of Lasser and Smith,[21] listed in Table I. The bands are numbered beginning with the lowest d band as band 1. The resulting spectra are shown in Figs. 8–10. The notation in the figures, e.g., 6-5L, refers to radiative recombination of electrons in band 6 (sp conduction band) with holes in band 5 (top d band), near the L symmetry point. In the spectral range we have studied, we only need to calculate luminescence from the radiative recombination of electrons in band 6 with the scattered holes in the d bands. The decrease in the luminescence at low energies results from a diminishing hole population [the exponential term in Eq. (5)], and the dispersion of the factor F (Fig. 7). Because of the many approximations used in this calculation, we

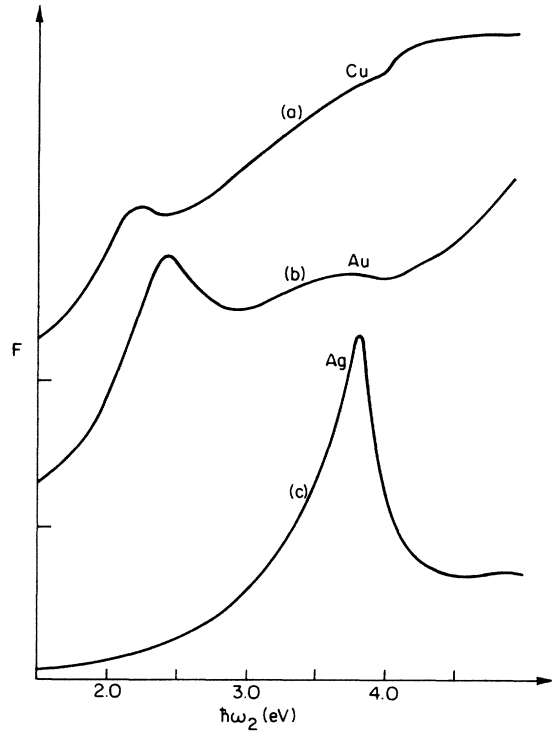

FIG. 7. Effects of the Fresnel coefficients and the absorption of the outgoing light on the one-photon-induced luminescence from the smooth surface are seen in the plot of the Fresnel factor [defined in the text following Eq. (6)], $F=\omega_2\,|L(\omega_1)|^2\,|L(\omega_2)|^2 z_0(\omega_1,\omega_2)$ versus ω_2, for $\hbar\omega_1=3.50$ eV.

TABLE I. Band parameters used in the calculation derived from Ref. 22. Masses are in units of the electron mass. The energy Δ is in eV.

Band (symmetry point)	Au Δ	Au m_1	Au m_2	Cu Δ	Cu m_1	Cu m_2	Ag Δ	Ag m_1	Ag m_2
6 (L)	−1.27	−0.174	0.225	−1.22	−0.182	0.341	−0.65	−0.30	−0.474
(X)	0.91	−0.162	0.300	1.90	−0.195	0.366			
5 (L)	−2.20	−1.74	−1.49	−2.02	−1.49	−5.0	−4.05	−2.73	−4.8
(X)	−1.86	−1.46	−1.40	−1.85	−3.80	−5.0			
4 (L)	−2.73	−0.507	−0.544	−2.15	−0.564	−0.690	−4.10	−2.27	−1.21
(X)	−2.59	−1.28	−1.04	−1.97	−3.2	−2.06			
3 (L)	−4.46	3.7	−4.2	−3.40	5.0	3.8			
(X)	−2.97	−1.79	−0.744	−2.08	−4.0	−1.02			
a (Å)		4.06			3.61			4.09	

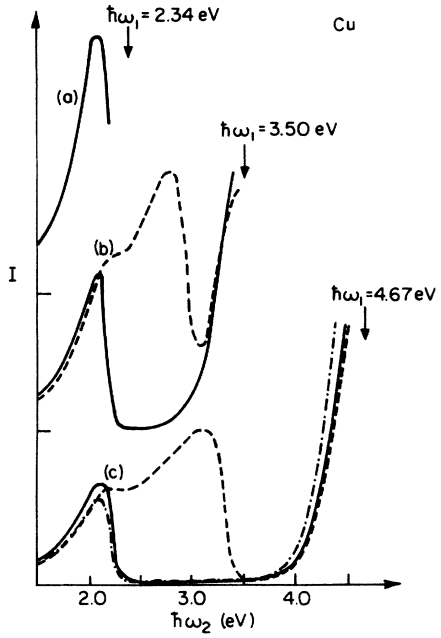

FIG. 8. Calculated one-photon-induced luminescence spectra for smooth Cu for excitation energies of (a) 2.34, (b) 3.50, and (c) 4.67 eV. Solid line denotes 6-5L transitions, dashed line denotes 6-4L transitions, and dashed-dotted line denotes 6-3X transitions.

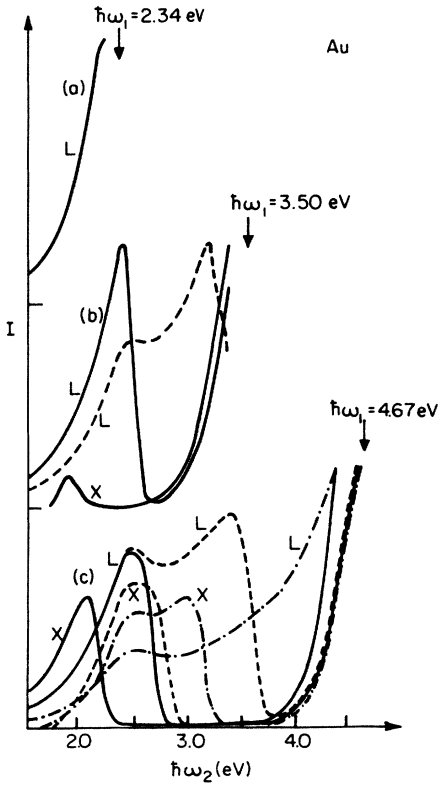

FIG. 9. Calculated one-photon-induced luminescence spectra for smooth Au for excitation energies of (a) 2.34, (b) 3.50, and (c) 4.67 eV. Solid line denotes 6-5 transitions, dashed line denotes 6-4 transitions, and dashed-dotted line denotes 6-3 transitions.

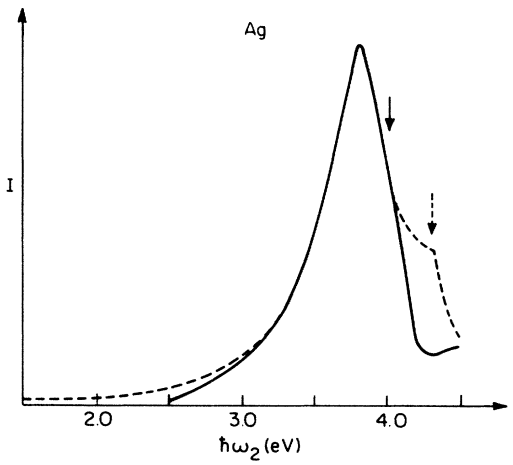

FIG. 10. Calculated one-photon-induced luminescence spectrum for smooth Ag for the excitation energy of 4.67 eV. Vertical arrows indicate the position of two peaks resulting from the 6-5L transition (——) and the 6-4L transition (— — —).

should not take the calculated spectrum too seriously, but simply focus our attention on the peak positions.

1. Copper

The calculated luminescence peak, at ~2.0 eV shown in Fig. 8(a) for Cu for the excitation energy of 2.34 eV, results from transitions from band 6 to band 5 near the L symmetry point. The position of the peak is within 0.1 eV of that measured from the smooth sample [Fig. 2(a)], and is well within the accuracy of the band-structure parameters from Table I. At the excitation of 3.50 eV, holes are also created in the second-highest d band (4), giving rise to the second major peak at 2.7 eV in Fig. 8(b), also in good agreement with observation from the smooth sample [Fig. 2(b)]. The calculated rise in intensity near the excitation energy results from recombination of holes and electrons near their initial excitation energies. This is also evident in the measured spectrum in Fig. 2(b).

The calculated spectrum with 4.67 eV excitation is shown in Fig. 8(c). There is a transition from a lower d band (3) near the X symmetry point which contributes a peak near that of the 6-5L transition. Because an experimental spectrum is not available in this case, no comparison between theory and experiment can be made.

2. Gold

The calculated luminescence spectrum for smooth Au, excited at 2.34 eV, is shown in Fig. 9(a). This energy is just sufficient to promote electrons from the top d band to the Fermi level near L. Consequently, the spectrum shows only part of a peak. The calculation is in reasonable agreement with the data in Fig. 3(a). For the excitation energy of 3.50 eV, the full peak of the 6-5L transition at 2.4 eV is evident in Fig. 9(b), along with peaks at 3.1 and 1.9 eV from the 6-4L and 6-5X transitions, respectively. The shoulder at 2.4 eV in the 6-4L contribution is

due to dispersion of the Fresnel factor [Fig. 7(b)]. The observed peaks in the luminescence spectrum from the smooth sample of Au [Fig. 3(b)], differ from the 2.4- and 3.1-eV peaks in the calculation by less than 0.1 and 0.3 eV, respectively, which is within the accuracy of the band parameters used. The weak structure in the data near 1.9 eV correlates with the calculated peak position of the 6-5X transition.

At the excitation energy of 4.67 eV, many more transitions, become possible in Au, as is evident in Fig. 9(c). A comparison of this figure with the measured spectrum in Fig. 3(c) leads to the following assignments: The main peak at 3.1 eV in the experiment appears to be a composite of the 6-4L and 6-3X transitions. The smaller peak at 2.2 eV is a combination of the 6-5L and 6-4X transitions, while the weaker structure near 1.9 eV may correspond to the 6-5X transition. The rise in the luminescence near the excitation energy is again attributed to recombination of electrons and holes near their initial excitation energies.

3. Silver

For the excitation of 4.67 eV, Eq. (6) predicts luminescence peaks for Ag at 4.0 and 4.3 eV, resulting from the 6-5L and 6-4L transitions, respectively. Unlike Cu and Au, however, the Fresnel factor shows a pronounced peak [Fig. 7(c)] at the volume-plasmon resonance energy, which masks over these interband peaks. The calculated spectrum is shown in Fig. 10. The positions of the interband transition peaks are indicated by the vertical arrows in the figure. The calculation is in reasonable agreement with the measured spectrum from the smooth sample (Fig. 4). The step in the data above 4 eV corresponds with the calculated step due to the 6-4L transition at 4.3 eV.

The measured peak actually appears to be shifted by ≈ 0.1 eV below the volume-plasmon energy of 3.8 eV. This lower-energy cutoff of the peak is likely due to the surface-plasmon resonance at the Ag-vacuum interface [$\mathrm{Re}(\epsilon_m)=-1$]. There is ample evidence in the literature[26,29] suggesting that coupling between radiative fields and surface plasmons can occur on evaporated Ag films via grain-boundary scattering. The peak we observe from Ag at ~ 3.7 eV may therefore result from luminescence via combined volume- and surface-plasmon emission. To our knowledge, such a photoinduced plasmon emission from a vacuum-metal interface has never been reported.

Whittle and Burstein[30] have suggested that this peak results from electron-hole recombination between two conduction bands, namely 7-6L. However, photoabsorption from band 6 to band 7 is relatively weak in Ag.[25] An examination of the calculated band structures for Ag (Ref. 21) further shows that electrons photoexcited into the upper conduction band should relax to a minimum at L, after which direct recombination would yield a peak near 4.3 rather than 3.7 eV.

C. Effects of roughness on the surface local fields

From SERS and surface-enhanced SHG studies,[4,20,28] it is known that an important effect of surface roughness is the enhancement of the incoming and outgoing fields via local plasmon resonances. For the smooth surfaces, the Fresnel factors $L(\omega_1)$ and $L(\omega_2)$ were used to account for the changes in the incoming and outgoing fields after crossing the metal surface. These factors may be thought of as macroscopic local-field correction factors, which can also be derived for a rough surface.[28] A simple model can be used to approximate a rough surface, and has been successfully applied to the analysis of surface-enhanced Raman scattering, absorption, and SHG results.[4,20,28] The rough surface is assumed to be a random collection of noninteracting hemispheroids of dielectric constant ϵ_m, siting perpendicularly on an infinitely conducting plane. The local field factors for each hemispheroid, L_{sph}, will be a function of ϵ_m, their height a, and radius b. From Ref. 28, we have for the local-field factor within the spheroid,

$$L_{\mathrm{sph}}(\omega)=A^{-1}\{\epsilon_m(\omega)-1 + A^{-1}[1+i4\pi^2 V(1-\epsilon_m(\omega))/3\lambda^3]\}^{-1}, \tag{12}$$

where the depolarization factor

$$A=1-\xi Q_1'(\xi)/Q_1(\xi),$$

$$\xi=[1-(b/a)^2]^{-1/2},$$

$$Q_1(\xi)=(\xi/2)\ln[(\xi+1)/(\xi-1)]-1,$$

$$Q_1'(\xi)=dQ_1(\xi)/d\xi,$$

λ is the optical wavelength, and $V=4\pi ab^2/3$ is the spheroid volume. The emitted single-photon luminescence power from the volume of the hemispheroid is then

$$P_{1\mathrm{sph}}(\omega_2, a/b, V)=\beta_1 2^4 |\mathbf{E}_0|^2 V[L^2(\omega_1)L^2(\omega_2)]_{\mathrm{sph}}, \tag{13}$$

where β_1 is a proportional constant which includes the intrinsic luminescence spectrum, and $\mathbf{E}_0$ is the incident electric field. The effects of spheroid shape on the dispersion of P_1 may be seen in a plot of P_1/β_1 versus $\hbar\omega_2$ and a/b.

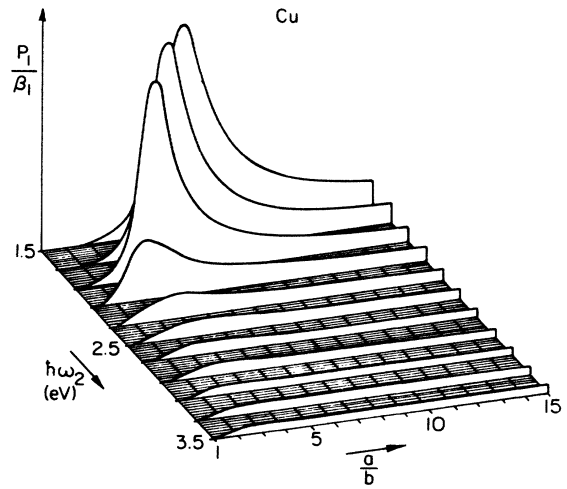

FIG. 11. Calculated single-photon-induced luminescence power, $P_{1\mathrm{sph}}/\beta_1$ from Cu hemispheroids of height a and radius b, versus a/b and the emission energy $\hbar\omega_2$, with $\hbar\omega_1=3.50$ eV.

Figure 11 shows such a plot for Cu spheroids with $\hbar\omega_1=3.50$ eV. We see from the figure that each emission energy is resonantly enhanced within a specifically shaped spheroid. At progressively lower emission energies, the resonance shifts to more prolate spheroids, where the so-called "lightning-rod" effect increases the local-field enhancement.[20] At emission energies above the interband absorption edge, the plasmon resonance is significantly damped (near 2 eV for Cu), resulting in a sharp drop in P_1.

We compare the luminescence from the rough surface to that from a smooth surface. The one-photon-induced luminescence power emitted from the bulk of a smooth metal can be rewritten from Eq. (6) as

$$P_{1\text{plane}}(\omega_2)=\beta_1 |\mathbf{E}_0|^2 Az_0\omega_2 |L^2(\omega_1)L^2(\omega_2)|_{\text{plane}}, \quad (14)$$

in which A is the illuminated area. Assuming that the smooth and rough surfaces differ only in their L factors, the one-photon luminescence enhancement from a single type of spheroids will be

$$\eta_1=N(a/b,V)P_{1\text{sph}}/P_{1\text{plane}},$$

where $N(a/b,V)$ is the number of spheroids of volume V and aspect ratio a/b within a specified interval $\pm\Delta V$ and $\pm\Delta(a/b)$. To obtain the total luminescence enhancement, we sum η_1 over a distribution of a/b and V which simulates our rough surfaces. From Eqs. (13) and (14) the total enhancement becomes

$$\eta_{1T}(\omega_1,\omega_2)=\sum_{a/b,\,V}\{[N(a/b,V)/A]2^4V[L^2(\omega_1)L^2(\omega_2)]_{\text{sph}}/[z_0L^2(\omega_1)L^2(\omega_2)]_{\text{plane}}\}. \quad (15)$$

We make the approximation that all shapes are equally probable, so that the factor N/A in Eq. (15) can be taken out of the sum. The factor N/A represents an effective shape density, and may be used to characterize the rough samples. It may be determined by comparing the calculated sum $\eta_{1T}/(N/A)$ with the luminescence enhancement, defined as the ratio of the single-photon luminescence from the rough samples to that from the smooth.

The effects of local-field enhancement is expected to be more pronounced for the multiphoton-induced luminescence, because of the higher power dependence in the incident field. The largest fields on the rough samples will be at the surface of the metal protrusions, being roughly $\epsilon_m/2$ times the fields in the metal bulk. If we consider, for example, the two-photon-induced luminescence from the surface atoms, over a thickness t on a metal spheroid, and compare it to that from the spheroid volume, we have

$$\frac{P_{2\text{surf}}}{P_{2\text{vol}}}\approx\frac{[L^4_{\text{sph}}(\omega_1)L^2_{\text{sph}}(\omega_2)abt]_{\text{surf}}}{[L^4_{\text{sph}}(\omega_1)L^2_{\text{sph}}(\omega_2)ab^2]_{\text{vol}}}$$
$$\approx 2^{-6}\epsilon_m^4(\omega_1)\epsilon_m^2(\omega_2)t/b.$$

For $\hbar\omega_1=1.17$ eV, $\hbar\omega_2=2$ eV, and $t/b=0.05$, $P_{2\text{surf}}/P_{2\text{vol}}\approx 300$ for Au and Cu, and 1.4×10^3 for Ag. Thus, although the volume contains more atoms, the local-field enhancement is sufficient to make the contribution from the surface atoms dominate. A similar estimate for one-photon-induced luminescence yields $(P_{1\text{sph}})_{\text{surf}}/(P_{1\text{sph}})_{\text{vol}}=0.2$, 0.3, and 1.6 for Au, Cu, and Ag, respectively ($\hbar\omega_1=2.34$ eV, $\hbar\omega_2=2.0$ eV), indicating that the surface contribution is less important.

The complete expression for the two-photon-excited luminescence power from a single hemispheroid comes after integrating the fields over its surface:

$$P_2=\beta_2|\mathbf{E}_0|^4 f(a/b)b^2t[(L')^4(\omega_1)(L')^2(\omega_2)]_{\text{sph}}, \quad (16)$$

where β_2 incorporates the intrinsic luminescence spectrum, and $L'_{\text{sph}}(\omega)=\epsilon_m L_{sph}(\omega)$. The geometric factor $f(a/b)$ is

$$f(a/b)=\xi^5(b/a)^5\{(5\xi^2/2)\cos^{-1}(b/a)$$
$$+(a/b)^3[10/3\xi-1/2\xi^2-5\xi/2]\}$$
$$\sim(b/a)^2/3 \quad (a\gg b). \quad (17)$$

The effects of the spheroid shape on the dispersion of P_2 may be seen in the plot of P_2/β_2 in Fig. 12 for Cu, using $\hbar\omega_1=1.17$ eV. Since P_2 is dependent on $(L')^4_{\text{sph}}(\omega_1)$, the luminescence predominantly emanates from spheroids resonant at ω_1, here at $a/b=10.0$. The plasmon resonance at ω_1 will significantly modify the intrinsic multiphoton luminescence spectrum, causing the intensity to rise near ω_1, and drop above the interband absorption edge (≈ 2 eV for Cu) where the plasmon resonance is damped.

We sum P_2 over all values of a/b and V, as was done for the single-photon excitation. We designate the total two-photon-induced luminescence power as

$$P_{2T}=\sum_{a/b,\,V}N(a/b,V)P_2(a/b,V). \quad (18)$$

In addition, we obtain for the two-photon luminescence enhancement,

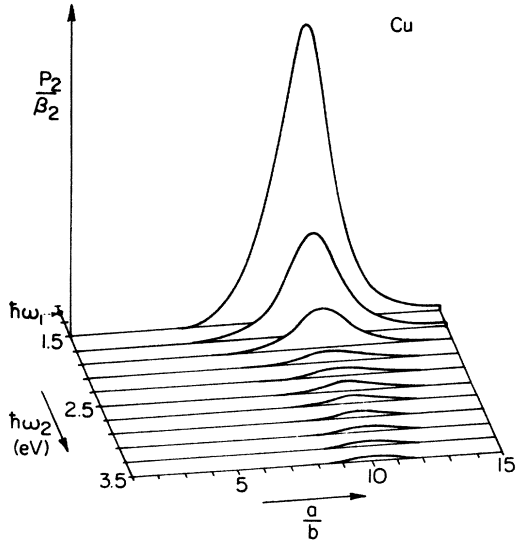

FIG. 12. Calculated P_2/β_2, as defined in Eq. (16), for Cu hemispheroids of height a and radius b, versus a/b and the emission energy $\hbar\omega_2$, with $\hbar\omega_1=1.17$ eV.

$$\eta_{2T}=\sum_{a/b,\,V}\pi 2^7(N/A)f(a/b)b^2[(L')^4(\omega_1)(L')^2(\omega_2)]_{\rm sph}/[(L')^4(\omega_1)(L')^2(\omega_2)]_{\rm plane}, \tag{19}$$

where[28]

$$L'_{\rm plane}(\omega)=2\epsilon_m^{1/2}(\omega)\cos\theta/[\epsilon_m^{1/2}(\omega)\cos\theta+\cos\theta_m]\ . \tag{20}$$

D. Comparisons with the luminescence from the rough surfaces

In this subsection the local-field calculations of subsection C are compared with the measured one-photon luminescence enhancement, and with the multiphoton luminescence spectra of the rough surfaces of noble metals.

1. Single-photon excitation

a. Copper. The measured surface enhancement of the luminescence spectrum, which is the ratio of the one-photon-excited spectra from the rough and smooth samples, is compared with the predictions of Eq. (15) for Cu in Figs. 13(a) and 13(b). For the excitations of 2.34 and 3.50 eV, we deduce a value for $N/A\approx 0.2/\mu m^2$, using the optimum spheroid volume in the calculation, and $\Delta(a/b)=1$. From electron photomicrographs of our rough surfaces, this value for N/A is quite reasonable. The dispersion of the enhancement is in good agreement with the predictions of the spheroid model of the rough surface. Little or no enhancement is predicted for $\hbar\omega_2>2.2$ eV, due to the damping of the localized plasmon resonances. Below this energy, the rise in η_{1T} is due to a shift of the resonances to more prolate structures which show stronger enhancement due to the lightning-rod effect.

A similar dispersion in the enhancement is expected for the excitation at 4.67 eV [Fig. 14(a)]. However, because an experimental spectrum from the smooth surface is not available, we cannot make a comparison between the theoretical and experimental enhancements. We see from Fig. 14(a) that the local-field enhancement should only affect the luminescence spectrum below 2.2 eV. The spectrum from the rough surface [Fig. 2(c)] shows peaks at 2, 2.4, and 3 eV, in addition to a rise in intensity near the excitation. With the exception of the 2.4-eV peak, the agreement with the peak positions from the analysis for the smooth surface [Fig. 8(c)] is satisfactory. The origin of the 2.4-eV peak is unknown.

b. Gold. The measured and calculated single-photon luminescence enhancements for Au are compared in Figs. 13(c) and 13(d). We deduce a value for N/A from the comparison, for both the 2.34- and 3.50-eV excitations, which is approximately one-fourth the value obtained for Cu. This discrepancy is in spite of the fact that the same roughened substrate was used for both metals, implying similar morphologies, and that the calculated resonant values for a/b were also approximately the same. Because of the crudity of the rough-surface model, however, close agreement for the absolute value of N/A is not expected. The dispersion of the luminescence enhancement is in reasonable agreement with the local-field calculation. The predicted leveling off above 2.2 eV results from the damping of the plasmon resonances. Essentially the same dispersion is predicted for the surface enhancement with the 4.67 eV excitation, but is different from what we observed [Fig. 14(b)]. The order-of-magnitude decrease in the rise in the luminescence near the excitation can be modeled by a decrease in δ_e and δ_h in the electron and

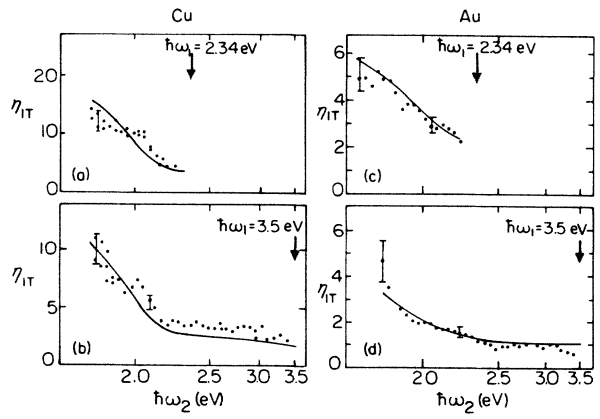

FIG. 13. Ratio of the measured one-photon-induced luminescence from the rough samples to that from the smooth (dots), compared with the prediction (solid curves).

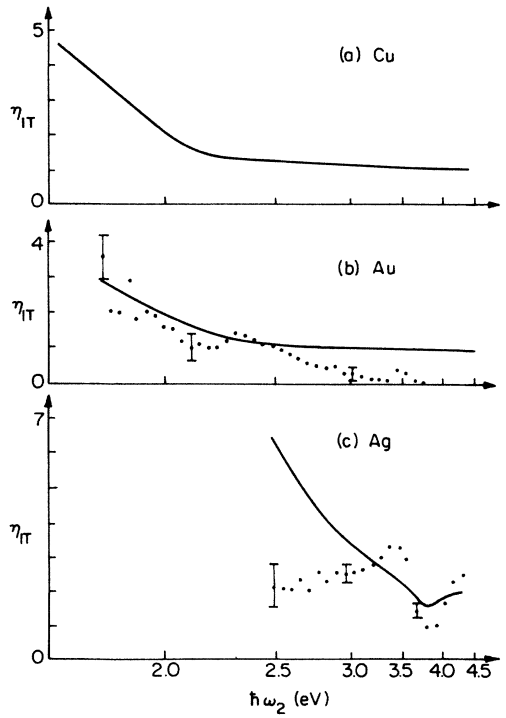

FIG. 14. Ratio of the measured one-photon-induced luminescence from the rough samples to that from the smooth (dots) compared with the prediction (solid curves), for $\hbar\omega_1=4.67$ eV. The ratio could not be obtained for Cu.

hole distributions in Eqs. (4) and (5). This implies a more rapid energy decay of the carriers, perhaps induced by more frequent collisions with the rough surface. A decrease in these exponential widths, however, does not explain the suppression of the luminescence peak near 3.2 eV. It is unknown why this peak, assigned to the 6-4L and 6-3X transitions, is suppressed by roughness.

c. Silver. For $\hbar\omega_1 = 4.67$ eV, Eq. (15) predicts a single-photon luminescence enhancement for Ag which rises monotonically with decreasing emission energy [Fig. 14(c)]. However, the actual ratio of the spectra from the rough and smooth samples of Ag shows an enhancement which levels off below 3.3 eV. It seems that surface roughness on Ag is more effective in enhancing and extending the surface-plasmon emission to lower energies via increased momentum scattering[26,29] than enhancing luminescence via local plasmon resonances. This effect has already been observed for Ag in surface-plasmon emission induced by electron bombardment.[31] The low-energy cutoff we observed in the rough-sample spectrum is then related to the limit in scattering momentum available from our roughened surface.

2. Multiphoton excitation

Unlike the single-photon-induced luminescence, multiphoton luminescence could not be detected from the smooth surfaces with our detection system. This sets a lower limit for the enhancement of approximately 10^2 for all the metals. On the other hand, we may estimate the two-photon luminescence enhancement from Eq. (19). Using $\hbar\omega_1 = 1.17$ eV, and the values already deduced for N/A, we find $\eta_{2T} \approx 10^8$ for Ag and $\eta_{2T} \approx 10^6$ for Cu and Au. Thus, the multiphoton-induced luminescence is not likely to be detected without the local-field enhancement. The effect of the rough surface on the dispersion of the multiphoton luminescence may be estimated from Eqs. (16)–(18). The results of the calculation are compared with the measured spectra in Figs. 15 and 16.

The plot of the calculated spectrum $P_{2T}(\omega_2)$ from Eq. (18) for Cu is shown as a solid curve in Fig. 15(a). The rise in intensity with decreasing emission energy results from the resonance at ω_1 discussed in Sec. IV C. The leveling off of P_{2T} near the interband absorption edge is due to the damping of the plasmon oscillations. The same behavior is observed in the measured spectrum shown as a dashed curve in the same figure. In a similar calculation of the two-photon luminescence originating from the bulk of the spheroids, only a very gradual rise in intensity with decreasing ω_2 is predicted. This is consistent with an earlier conclusion in subsection C that the enhanced multiphoton luminescence predominantly emanates from the surface atoms of the rough structures. The one-photon luminescence, on the other hand, is more likely to originate from the bulk. This could explain the lack of a luminescence peak in the two-photon-excited spectrum from Cu, since the dispersion of the surface enhancement strongly dominates, and since the spectra from the surface and bulk atoms may be very different. It has also been suggested that the peak is missing because of two-photon selection rules.[17] However, we do not expect the band

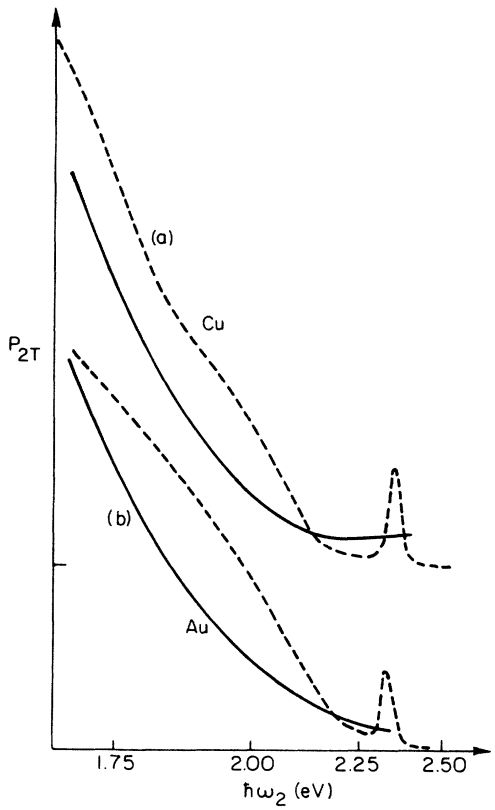

FIG. 15. Solid curves indicate the calculated two-photon-induced luminescence power from a distribution of spheroids, P_{2T}, versus the emission energy $\hbar\omega_2$, using $\hbar\omega_1 = 1.17$ eV. The dashed curves are the measured spectra from Fig. 5.

parities to be so well defined as to forbid direct two-photon absorption at transitions allowed for one-photon excitation.

A plot of the calculated $P_{2T}(\omega_2)$ for Au, using $\hbar\omega_1 = 1.17$ eV, is shown as a solid curve in Fig. 15(b). As with Cu, the local-field dispersion for the surface atoms

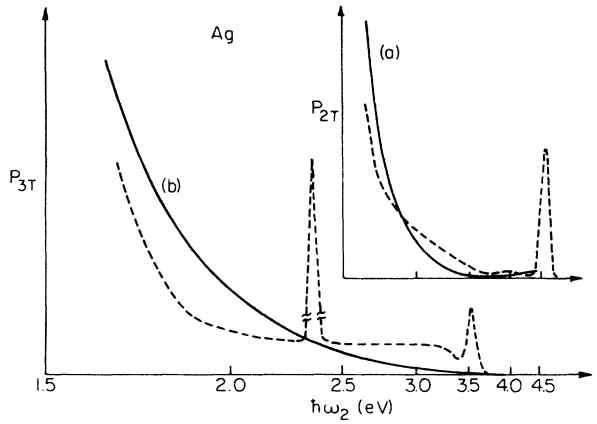

FIG. 16. Solid curves indicate (a) the calculated two-photon-induced luminescence power from a distribution of spheroids, P_{2T}, versus the emission energy $\hbar\omega_2$, for Ag with $\hbar\omega_1 = 2.34$ eV, and (b) the three-photon-induced luminescence power, P_{3T}, for $\hbar\omega_1 = 1.17$ eV. The dashed curves are the measured spectra from Fig. 5.

of the spheroid corresponds with the observed luminescence spectrum (dashed curve). The same calculation for emission from the spheroid bulk gives a much more gradual rise. We conclude, as with Cu, that the two-photon-induced luminescence emanates predominantly from the surface atoms of the roughness protrusions.

The solid curve in Fig. 16(a) is a plot of the calculated $P_{2T}(\omega_2)$ for Ag, for $\hbar\omega_1=2.34$ eV. As with Cu and Au, the observed rise in intensity with decreasing emission energy is predicted by the local-field model, assuming emission is predominantly from the surface atoms. The dip in $P_{2T}(\omega_2)$ near the volume-plasmon energy of 3.8 eV results from a decrease in the fields at the surface as $\mathrm{Re}(\epsilon_m)=0$. This reduction in the local-field enhancement may be the reason why no peak exists at this energy in the measured two-photon luminescence spectrum [Fig. 5(d)].

For $\hbar\omega_1=1.17$ eV, the observed multiphoton-excited spectrum from rough Ag extends out to the three-photon energy [Fig. 5(c)]. Assuming that the luminescence was induced by three-photon excitation, we computed the emitted luminescence power, as in subsection C, from the surface of a distribution of spheroids. The result, designated as $P_{3T}(\omega_2)$, is plotted as a solid curve in Fig. 16(b). The rise in the luminescence with decreasing emission energy is again predicted. We note that because the dispersion of this curve results from the localized plasmon resonance at ω_1, we obtain qualitatively the same result as for $P_{2T}(\omega_2)$.

We have estimated that the enhancement of the three-photon luminescence exceeds that of the two-photon luminescence by $\sim 10^5$ for Ag, but only by $\sim 10^4$ Au and Cu, for $\hbar\omega_1=1.17$ eV. This may help to explain why the luminescence is very weak at energies above $2\omega_1$ for Au and Cu.

V. CONCLUSIONS

The luminescence spectra induced by single-photon absorption from the smooth noble metals display pronounced structures. A detailed calculation qualitatively reproducing most of the observed structures suggests that the peaks in Cu and Au result from direct radiative recombination of electrons below the Fermi level with holes in the d bands around the X and L symmetry points. The decrease in the luminescence on the low-energy side of the peaks results from a diminishing hole population in the d bands, and a decrease in the transmission coefficient of the outgoing light. The rise in the luminescence intensity near the excitation energy is believed to originate from radiative recombination of electrons and holes near their initially excited energies. In contrast to Cu and Au, the single-photon-excited luminescence spectrum from Ag appears to be dominated by radiative emission of the surface and volume plasmons.

Many of the effects or roughness on the single-photon-excited spectra may be attributed to the effects of localized plasmon resonances. In particular, the enhancement of the luminescence by such resonances begins only at emission energies below the interband absorption edge of the metal, where the plasmon oscillations are less damped. However, the observed suppression of certain spectral features when the surfaces are roughened cannot be explained by a simple local-field theory for the rough surface. We suggest that the roughness may somehow quench the luminescence, for example, by increasing the nonradiative recombination rate, perhaps via collisions with the rough surface.

For the multiphoton-excited spectra from the rough samples, we observe a monotonic rise in the luminescence intensity with decreasing emission energy, and an absence of the peaks which characterize the single-photon spectra. An analysis of the effects of local-field enhancement shows that the multiphoton luminescence is emitted predominantly from the surface atoms of protrusions on the rough surface with localized plasmon resonances at ω_1. The rise in the luminescence intensity towards lower energies is attributed to this resonance. The peak near 2 eV in the one-photon luminescence spectrum from Cu is believed to be missing from the two-photon spectrum, because of an intrinsic difference in the luminescence of the surface atoms from that of the bulk. For Ag, the peak at 3.7 eV is believed to be missing from the two-photon spectrum because of a drop in the local-field enhancement at this energy, at the surface of the protrusions, as $\mathrm{Re}(\epsilon_m)=0$.

As we see, the uncertainties in the population distribution of the electrons and holes, and the various local-field effects, complicate the interpretation of the spectra. This limits the use of photoluminescence as a band-structure probe. One could, however, obtain far more complete band-structure information if the excitation frequency ω_1 could be scanned continuously to yield a series of luminescence spectra. Despite the limitations of the present photoluminescence technique, it may still prove useful in complementing the data from other techniques, such as photoabsorption and photoemission, for studying the electronic properties of metals.

ACKNOWLEDGMENT

This work was supported by the Director, Office of Energy Research, Office of Basic Energy Sciences, Materials Sciences Division of the U.S. Department of Energy under Contract No. DE-AC03-76SF00098.

*Present address: 3M Research Laboratories, St. Paul, MN 55144-1000.

[1]A. Mooradian, Phys. Rev. Lett. 22, 185 (1969).

[2]Some qualitative details of the luminescence mechanism are discussed in D. Whittle, Ph.D. thesis, University of Pennsylvania, 1982 (unpublished).

[3]L. M. Fraas and S. P. S. Porto, in *Proceedings of the Second International Conference on Light Scattering in Solids* (Flammarion, Paris, 1971), p. 90.

[4]See, for example, *Surface Enhanced Raman Scattering,* edited by R. K. Chang and T. E. Furtak (Plenum, New York, 1982); M. Moskovits, Rev. Mod. Phys. 57, 783 (1985).

[5]J. P. Heritage, J. G. Bergman, A. Pinczuk, and J. M. Worlock, Chem. Phys. Lett. **67**, 229 (1979).
[6]I. Pockrand and A. Otto, Solid State Commun. **37**, 109 (1981).
[7]I. Pockrand and A. Otto, Appl. Surf. Sci. **6**, 362 (1980).
[8]H. Seki, J. Chem. Phys. **76**, 4412 (1982).
[9]A. M. Glass, P. F. Liao, J. G. Bergman, and D. H. Olson, Opt. Lett. **5**, 368 (1980).
[10]A. M. Glass, A. Wokaun, J. P. Heritage, J. G. Bergman, P. F. Liao, and D. H. Olson, Phys. Rev. B **24**, 4906 (1981).
[11]G. M. Goncher and C. B. Harris, J. Chem. Phys. **77**, 3767 (1982).
[12]J. Lambe and S. L. McCarthy, Phys. Rev. Lett. **37**, 923 (1976).
[13]A. Adams and P. K. Hansma, Phys. Rev. B **23**, 3597 (1981).
[14]P. Dawson, D. G. Walmsley, H. A. Quinn, and A. J. L. Ferguson, Phys. Rev. B **30**, 3164 (1984).
[15]C. K. Chen, A. R. B. de Castro, and Y. R. Shen, Phys. Rev. Lett. **46**, 145 (1981).
[16]G. T. Boyd, Z. H. Yu, and Y. R. Shen, Bull. Am. Phys. Soc. **27**, 377 (1982).
[17]D. Whittle and E. Burstein, Bull. Am. Phys. Soc. **29**, 480 (1984).
[18]W. M. H. Sachtler, G. J. H. Dorgelo, and A. A. Holscher, Surf. Sci. **5**, 221 (1966); P. C. Richardson and D. R. Rossington, J. Catal. **20**, 420 (1981); D. D. Eley and P. B. Moore, Surf. Sci. **76**, L599 (1978).
[19]L. F. Wagner and W. E. Spicer, Surf. Sci. **46**, 301 (1974); G. Rovida, F. Pratesi, M. Maglietta, and E. Ferroni, *ibid.* **43**, 230 (1974).
[20]G. T. Boyd, Th. Rasing, J. R. R. Leite, and Y. R. Shen, Phys. Rev. B **30**, 510 (1984).
[21]R. Lasser and N. V. Smith, Phys. Rev. B **24**, 1895 (1981); N. E. Christensen and B. O. Seraphin, *ibid.* **4**, 3321 (1971); H. Ehrenreich and H. R. Philipp, Phys. Rev. **128**, 1622 (1962).
[22]A. Girlando, W. Knoll, and M. R. Philpott, Solid State Commun. **38**, 895 (1981).
[23]P. B. Johnson and R. W. Christy, Phys. Rev. B **6**, 4370 (1972).
[24]R. Rosei, Phys. Rev. B **10**, 474 (1974); M. Guerri and R. Rosei, *ibid.* **12**, 557 (1975).
[25]H. G. Liljenvall and A. G. Mathewson, J. Phys. C Suppl. 3, S341 (1970).
[26]H. Raether, *Physics of Thin Films* (Academic, New York, 1977), Vol. 9, p. 38.
[27]M. Kaveh and N. Wiser, Adv. Phys. **33**, 257 (1984).
[28]C. K. Chen, T. F. Heinz, D. Ricard, and Y. R. Shen, Phys. Rev. B **27**, 1965 (1983).
[29]P. Dobberstein, A. Hampe, and G. Sauerbrey, Phys. Lett. **27A**, 256 (1968); E. Schröder, Z. Phys. **38**, 26 (1969); S. N. Jasperson and S. E. Schnatterly, Phys. Rev. **188**, 759 (1969).
[30]D. Whittle and E. Burstein, Bull. Am. Phys. Soc. **29**, 480 (1984).
[31]G. L. Eesley, Phys. Rev. B **24**, 5477 (1981).